

No-Core Shell Model Analysis of Light Nuclei

Sofia Quaglioni · Petr Navrátil ·
Guillaume Hupin · Joachim Langhammer ·
Carolina Romero-Redondo · Robert Roth

Received: date / Accepted: date

Abstract The fundamental description of both structural properties and reactions of light nuclei in terms of constituent protons and neutrons interacting through nucleon-nucleon and three-nucleon forces is a long-sought goal of nuclear theory. I will briefly present a promising technique, built upon the *ab initio* no-core shell model, which emerged recently as a candidate to reach such a goal: the no-core shell model/resonating-group method. This approach, capable of describing simultaneously both bound and scattering states in light nuclei, complements a microscopic

Computing support for this work came from the LLNL institutional Computing Grand Challenge program and the Jülich supercomputer Centre. Prepared in part by LLNL under Contract DE-AC52-07NA27344. Support from the U. S. DOE/SC/NP (Work Proposal No. SCW1158), the NSERC Grant No. 401945-2011, and from the U. S. Department of Energy Grant DE-FC02-07ER41457 is acknowledged. TRIUMF receives funding via a contribution through the Canadian National Research Council. This work is supported in part by the Deutsche Forschungsgemeinschaft through contract SFB 634 and by the Helmholtz International Center for FAIR within the framework of the LOEWE program launched by the State of Hesse.

Presented at the 20th International IUPAP Conference on Few-Body Problems in Physics, 20 - 25 August, 2012, Fukuoka, Japan

S. Quaglioni
Lawrence Livermore National Laboratory, P.O. Box 808, L-414, Livermore, CA 94551, USA
Tel.: +1-925-4228152
Fax: +1-925-4225940
E-mail: quaglioni1@llnl.gov

P. Navrátil
TRIUMF, 4004 Wesbrook Mall, Vancouver, BC V6T 2A3, Canada; Lawrence Livermore National Laboratory, P.O. Box 808, L-414, Livermore, CA 94551, USA

G. Hupin
Lawrence Livermore National Laboratory, P.O. Box 808, L-414, Livermore, CA 94551, USA

J. Langhammer
Institut für Kernphysik, Technische Universität Darmstadt, 64289 Darmstadt, Germany

C. Romero-Redondo
TRIUMF, 4004 Wesbrook Mall, Vancouver, BC V6T 2A3, Canada

R. Roth
Institut für Kernphysik, Technische Universität Darmstadt, 64289 Darmstadt, Germany

cluster technique with the use of two-nucleon realistic interactions, and a microscopic and consistent description of the nucleon clusters. I will discuss applications to light nuclei binary scattering processes and fusion reactions that power stars and Earth based fusion facilities, such as the deuterium- ^3He fusion, and outline the progress toward the inclusion of the three-nucleon force into the formalism and the treatment of three-body clusters.

PACS 24.10.-i · 24.10.Cn · 21.60.De · 25.40.Lw · 25.45.-z · 21.45.Ff

1 Introduction

Nuclei are aggregates of protons and neutrons interacting through forces arising from the underlying theory of quantum chromodynamics. Understanding how the strong force binds nucleons together in nuclei is fundamental to explain the very existence of the universe. Indeed, the mutual interactions between nucleons led to the formation of the lightest nuclei a few minutes after the Big Bang, and the following nuclear processes, producing heavier nuclei during stellar evolution and in violent events like supernovae, have been crucial in shaping the world we live in. Therefore, one of the central goals of nuclear physics is to come to a basic understanding of the structure and dynamics of nuclei. The *ab initio* (*i.e.* from first principles) no-core shell model/resonating group method (NCSM/RGM) [1, 2] is a theoretical technique that attempts to achieve such a goal for light nuclei.

2 *Ab initio* NCSM/RGM

In the *ab initio* NCSM/RGM approach the many-body wave function,

$$|\Psi^{J^\pi T}\rangle = \sum_{\nu} \int dr r^2 \hat{A}_{\nu} |\Phi_{\nu r}^{J^\pi T}\rangle \frac{[\mathcal{N}^{-1/2} \chi]_{\nu}^{J^\pi T}(r)}{r}, \quad (1)$$

is expanded over a set of translational-invariant cluster basis states describing two nuclei (a target and a projectile composed of $A-a$ and $a \leq A$ nucleons, respectively) whose centers of mass are separated by the relative coordinate $\mathbf{r}_{A-a,a}$ and that are traveling in a $^{2s}\ell_J$ wave or relative motion (with s the channel spin, ℓ the relative momentum, and J the total angular momentum of the system):

$$|\Phi_{\nu r}^{J^\pi T}\rangle = \left[(|A-a \alpha_1 I_1^{\pi_1} T_1\rangle |a \alpha_2 I_2^{\pi_2} T_2\rangle)^{(sT)} Y_{\ell}(\hat{r}_{A-a,a}) \right]^{(J^\pi T)} \frac{\delta(r - r_{A-a,a})}{r r_{A-a,a}}. \quad (2)$$

Here, the antisymmetric wave functions $|A-a \alpha_1 I_1^{\pi_1} T_1\rangle$ and $|a \alpha_2 I_2^{\pi_2} T_2\rangle$ are eigenstates of the $(A-a)$ - and a -nucleon intrinsic Hamiltonians, respectively, as obtained within the NCSM approach [3] and are characterized by the spin-parity, isospin and energy labels $I_i^{\pi_i}, T_i$, and α_i , respectively, where $i = 1, 2$. Additional quantum numbers labeling these RGM-inspired continuous basis states are parity $\pi = \pi_1 \pi_2 (-1)^{\ell}$ and total isospin T . In our notation, all these quantum numbers are grouped into a cumulative index $\nu = \{A-a \alpha_1 I_1^{\pi_1} T_1; a \alpha_2 I_2^{\pi_2} T_2; s\ell\}$. The Pauli

principle is enforced by introducing the appropriate inter-cluster antisymmetrizer, schematically

$$\hat{A}_\nu = \sqrt{\frac{(A-a)!a!}{A!}} \left(1 + \sum_{P \neq id} (-)^p P \right), \quad (3)$$

where the sum runs over all possible permutations of nucleons P different from the identical one that can be carried out between the two different clusters, and p is the number of interchanges characterizing them. Finally, the continuous linear variational amplitudes $\chi_\nu^{J^\pi T}(r)$ are determined by solving the orthogonalized RGM equations:

$$\sum_{\nu'} \int dr' r'^2 [\mathcal{N}^{-\frac{1}{2}} \mathcal{H} \mathcal{N}^{-\frac{1}{2}}]_{\nu\nu'}^{J^\pi T}(r, r') \frac{\chi_{\nu'}^{J^\pi T}(r')}{r'} = E \frac{\chi_\nu^{J^\pi T}(r)}{r}, \quad (4)$$

where $\mathcal{N}_{\nu\nu'}^{J^\pi T}(r, r')$ and $\mathcal{H}_{\nu\nu'}^{J^\pi T}(r, r')$, commonly referred to as integration kernels, are respectively the overlap (or norm) and Hamiltonian matrix elements over the antisymmetrized basis (2), *i.e.*:

$$\mathcal{N}_{\nu\nu'}^{J^\pi T}(r', r) = \langle \Phi_{\nu'r'}^{J^\pi T} | \hat{A}_{\nu'} \hat{A}_\nu | \Phi_{\nu r}^{J^\pi T} \rangle, \quad \mathcal{H}_{\nu\nu'}^{J^\pi T}(r', r) = \langle \Phi_{\nu'r'}^{J^\pi T} | \hat{A}_{\nu'} H \hat{A}_\nu | \Phi_{\nu r}^{J^\pi T} \rangle. \quad (5)$$

Here, H is the microscopic A -nucleon Hamiltonian and E is the total energy in the center of mass (c.m.) frame. For a detailed explanation of how norm and Hamiltonian kernels are obtained from the underlying nuclear interaction and the NCSM eigenvectors of target and projectile we refer the interested reader to Refs. [2] and [4].

3 Applications

Applications of the NCSM/RGM approach to the description of nucleon- and deuteron-nucleus type of collisions based on two-nucleon (NN) realistic interactions have already led to very promising results [1, 2, 5, 4, 6, 7]. In most instances, we employed similarity-renormalization-group (SRG) [8, 9] evolved potentials, and in particular, those obtained from the chiral $N^3\text{LO}$ [10] NN interaction. Here we briefly review two of such applications, the calculation of the ${}^7\text{Be}(p, \gamma){}^8\text{B}$ radiative capture [6], and the study of the ${}^3\text{H}(d, n){}^4\text{He}$ and ${}^3\text{He}(d, p){}^4\text{He}$ fusion reactions [7].

3.1 The ${}^7\text{Be}(p, \gamma){}^8\text{B}$ radiative capture

Recently, we have performed the first *ab initio* many-body calculation of the ${}^7\text{Be}(p, \gamma){}^8\text{B}$ radiative capture [6], the final step in the nucleosynthetic chain leading to ${}^8\text{B}$ and one of the main inputs of the Standard Solar Model. This calculation was carried out in a model space spanned by p - ${}^7\text{Be}$ channel states including the five lowest eigenstates of ${}^7\text{Be}$ (the $\frac{3}{2}^-$ ground and the $\frac{1}{2}^-$, $\frac{7}{2}^-$, and first and second $\frac{5}{2}^-$ excited states) in an $N_{\text{max}} = 10$ NCSM basis, and employed the SRG- $N^3\text{LO}$ NN interaction with $\Lambda = 1.86 \text{ fm}^{-1}$, where Λ denotes the SRG evolution parameter [8]. We first solved Eq. (4) with bound-state boundary conditions to find the

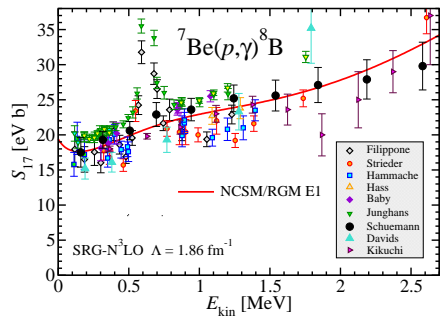


Fig. 1 Calculated ${}^7\text{Be}(p, \gamma){}^8\text{B}$ S-factor as a function of the energy in the center of mass compared to data. Only $E1$ transition were considered in the calculation.

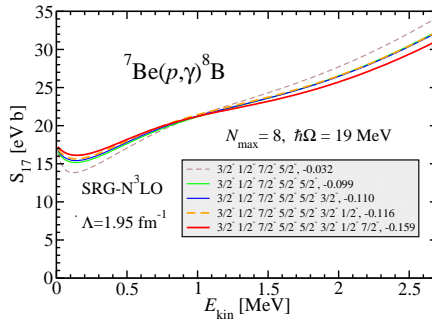


Fig. 2 Convergence of the ${}^7\text{Be}(p, \gamma){}^8\text{B}$ S-factor as a function of the number of ${}^7\text{Be}$ eigenstates included in the calculation (shown in the legend together with the corresponding separation energy).

bound state of ${}^8\text{B}$, and then with scattering boundary conditions to find the p - ${}^7\text{Be}$ scattering wave functions. Former and latter wave functions were later used to calculate the capture cross section, which, at solar energies, is dominated by non-resonant $E1$ transitions from p - ${}^7\text{Be}$ S - and D -waves into the weakly-bound ground state of ${}^8\text{B}$. All stages of the calculation were based on the same HO frequency of $\hbar\Omega = 18$ MeV, which minimizes the g.s. energy of ${}^7\text{Be}$.

At $N_{\text{max}} = 10$, the largest model space achievable for the present calculation within the full NCSM basis, the ${}^7\text{Be}$ g.s. energy is very close to convergence as indicated by a fairly flat frequency dependence in the range $16 \leq \hbar\Omega \leq 20$ MeV, and the vicinity to the $N_{\text{max}} = 12$ result obtained within the importance-truncated NCSM [11, 12]. With the chosen value $\Lambda = 1.86$ fm $^{-1}$ for the SRG evolution of the $N^3\text{LO}$ NN interaction, we obtain a single 2^+ bound state for ${}^8\text{B}$ with a separation energy of 136 keV, which is quite close to the observed one (137 keV). This is very important for the description of the low-energy behavior of the ${}^7\text{Be}(p, \gamma){}^8\text{B}$ astrophysical S-factor, known as S_{17} . While for a complete *ab initio* calculation one should include also the three-nucleon (NNN) interaction induced by the SRG evolution of the NN potential as well as the SRG-evolved attractive initial chiral NNN force, we note that in the Λ -range ~ 1.8 - 2.1 fm $^{-1}$, and, in very light nuclei, the former interaction is repulsive and the two contributions cancel each other to a good extent [13, 14].

Figure 1 compares the resulting S_{17} astrophysical factor with several experimental data sets. Energy dependence and absolute magnitude follow closely the trend of the indirect Coulomb breakup measurements of Shümann *et al.* [15], while somewhat underestimating the direct data of Junghans *et al.* [16]. The resonance due to the $M1$ capture, particularly evident in these and Filippone's data and missing in our results, does not contribute to a theoretical calculation outside of the narrow ${}^8\text{B}$ 1^+ resonance and is negligible at astrophysical energies [17]. The $M1$ operator, for which any dependence upon two-body currents needs to be included explicitly, poses more uncertainties than the Siegert's $E1$ operator. In addition, the treatment of this operator within the NCSM/RGM approach is slightly complicated by the contributions coming from the core (${}^7\text{Be}$) part of the wave function. Nevertheless, we plan to calculate its contribution in the future.

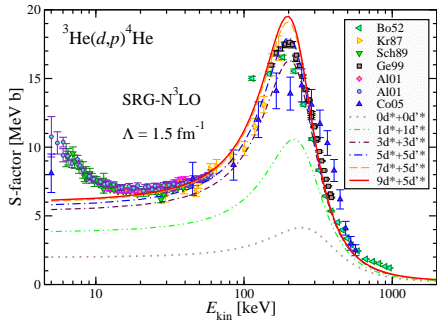


Fig. 3 Calculated S-factor of the ${}^3\text{He}(d,p){}^4\text{He}$ reaction compared to experimental data. Convergence with the number of deuterium pseudostates in the 3S_1 - 3D_1 (d^*) and 3D_2 (d'^*) channels.

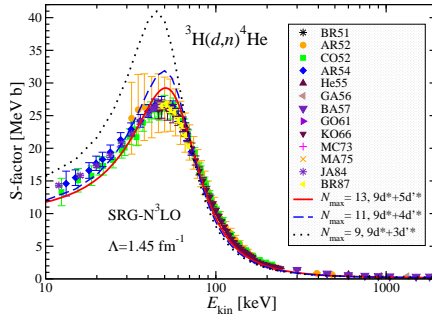


Fig. 4 Calculated ${}^3\text{H}(d,n){}^4\text{He}$ S-factor compared to experimental data. Convergence with N_{max} obtained for the SRG- N^3LO NN potential with $\Lambda = 1.45 \text{ fm}^{-1}$ at $\hbar\Omega = 14 \text{ MeV}$.

Our calculated $S_{17}(0) = 19.4(7) \text{ MeV b}$ is on the lower side, but consistent with the latest evaluation $20.8 \pm 0.7(\text{expt}) \pm 1.4(\text{theory})$ [17]. The 0.7 eV b uncertainty was estimated by studying the dependence of the S-factor on the harmonic oscillator (HO) basis size N_{max} as well as the influence of higher-energy excited states of the ${}^7\text{Be}$ target. More precisely, we performed calculations up to $N_{\text{max}} = 12$ within the importance-truncation NCSM scheme [11,12] including (due to computational limitations) only the first three eigenstates of ${}^7\text{Be}$. The $N_{\text{max}} = 10$ and 12 S-factors are very close. In addition, the convergence in the number of ${}^7\text{Be}$ states was explored by means of calculations including up to 8 ${}^7\text{Be}$ eigenstates in a $N_{\text{max}} = 8$ basis (larger N_{max} values are currently out of reach with more than five ${}^7\text{Be}$ states). This last set of calculations is presented in Fig. 2, from which it appears that, apart from the two $\frac{5}{2}^-$ states, the only other state to have a significant impact on the S_{17} is the second $\frac{7}{2}^-$, the inclusion of which affects the separation energy and contributes somewhat to the flattening of the S-factor around 1.5 MeV . For these last set of calculations we used SRG- N^3LO interactions obtained with different Λ values with the intent to match closely the experimental separation energy in each of the largest model spaces. Based on this analysis, we conclude that the use of an $N_{\text{max}} = 10$ HO model space is justified and the restriction to five ${}^7\text{Be}$ eigenstates is quite reasonable.

3.2 The ${}^3\text{H}(d,n){}^4\text{He}$ and ${}^3\text{He}(d,p){}^4\text{He}$ fusion reactions

In the following we present the first *ab initio* many-body calculations of ${}^3\text{H}(d,n){}^4\text{He}$ and ${}^3\text{He}(d,p){}^4\text{He}$ fusion reactions [7] starting from the SRG- N^3LO NN interaction with $\Lambda = 1.5 \text{ fm}^{-1}$, for which we reproduce the experimental Q -value of both reactions within 1%. These reactions have important implications first and foremost for fusion energy generation, but also for nuclear astrophysics, and atomic physics. Indeed, the deuterium-tritium fusion is the easiest reaction to achieve on earth and is pursued by research facilities directed at reaching fusion power. Both ${}^3\text{H}(d,n){}^4\text{He}$ and ${}^3\text{He}(d,p){}^4\text{He}$ affect the predictions of Big Bang nucleosynthesis for light-nucleus abundances. In addition, the deuterium- ${}^3\text{He}$ fusion is also an ob-

ject of interest for atomic physics, due to the substantial electron-screening effects presented by this reaction.

The model spaces adopted are characterized by HO model basis sizes up to $N_{\max} = 13$ with a frequency of $\hbar\Omega = 14$ MeV and channel bases including n - ${}^4\text{He}$ (p - ${}^4\text{He}$), d - ${}^3\text{H}$ (d - ${}^3\text{He}$), d^* - ${}^3\text{H}$ (d^* - ${}^3\text{He}$) and d'^* - ${}^3\text{H}$ (d'^* - ${}^3\text{He}$) binary cluster states. Here, d^* and d'^* denote 3S_1 - 3D_1 and 3D_2 deuterium excited pseudostates, respectively, and the ${}^3\text{H}$ (${}^3\text{He}$) and ${}^4\text{He}$ nuclei are in their ground state.

The results obtained for the ${}^3\text{He}(d,p){}^4\text{He}$ S-factor are presented in Figure 3. The deuteron deformation and its virtual breakup, approximated by means of d pseudostates, play a crucial role in reproducing the observed magnitude of the S-factor. Convergence is reached for $9d^* + 5d'^*$. The typical dependence upon the HO basis sizes adopted is illustrated by the ${}^3\text{H}(d,n){}^4\text{He}$ results of Fig. 4. The convergence is satisfactory and we expect that an $N_{\max} = 15$ calculation, which is currently out of reach, would not yield significantly different results. While the experimental position of the ${}^3\text{He}(d,p){}^4\text{He}$ S-factor is reproduced within few tens of keV and we find an overall fair agreement with experiment (if we exclude the region at very low energy, where the accelerator data are enhanced by laboratory electron screening), the ${}^3\text{H}(d,n){}^4\text{He}$ S-factor is not described as well with $\Lambda = 1.5$ fm $^{-1}$. Due to its very low activation energy, the ${}^3\text{H}(d,n){}^4\text{He}$ S-factor, particularly the position and height of its peak, is extremely sensitive to higher-order effects in the nuclear interaction, such as the NNN force (not yet included in the calculation) and missing isospin-breaking effects in the integration kernels (which are obtained in the isospin formalism). With a very small change in the value of the SRG evolution parameter we can compensate for these missing higher-order effects in the interaction and reproduce the position of the ${}^3\text{H}(d,n){}^4\text{He}$ S-factor. This led to the theoretical S-factor of Fig. 4 (obtained for $\Lambda = 1.45$ fm $^{-1}$), that is in overall better agreement with data, although it presents a slightly narrower and somewhat overestimated peak. This calculation would suggest that some electron-screening enhancement could also be present in the ${}^3\text{H}(d,n){}^4\text{He}$ measured S-factor below 10 keV c.m. energy. However, these results cannot be considered conclusive until more accurate calculations using a complete nuclear interaction (that includes the NNN force) are performed. Work in this direction is under way.

4 Recent developments

Here we outline some of our more recent efforts in the development of the NCSM/RGM approach, namely the progress toward the inclusion of the three-nucleon force into the formalism, and the treatment of three-body clusters and their dynamics.

4.1 Scattering and three-nucleon force

In past applications for light-ion reactions, we omitted the NNN interaction induced by the SRG renormalization of the NN potential as well as the initial chiral NNN force. By neglecting induced forces, we introduced a dependence on the SRG parameter Λ , which was then chosen so that the particle separation energies were well reproduced. For low-energy thermonuclear reactions, this is a dominant effect,

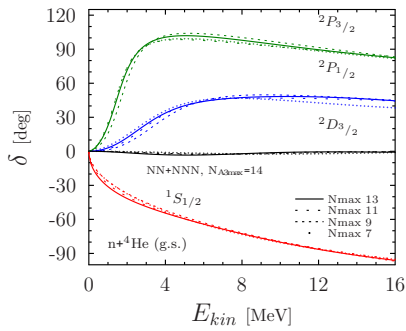


Fig. 5 Convergence with respect to the HO basis size $N_{\max} = 11$ at $\hbar\Omega = 20$ MeV of the $n+{}^4\text{He}(\text{g.s.})$ phase shifts obtained for the SRG- $(\text{N}^3\text{LO NN} + \text{N}^2\text{LO NNN})$ interaction with $\Lambda = 2.0 \text{ fm}^{-1}$. The label $N_{A3\max} = 14$ refers to the HO size of the NNN matrix elements.

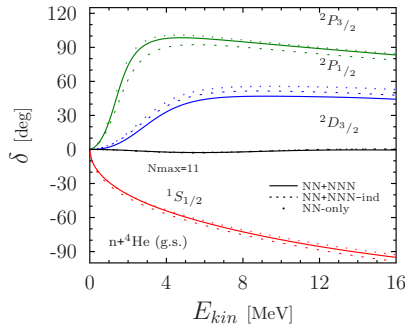


Fig. 6 Calculated $n+{}^4\text{He}(\text{g.s.})$ phase shifts for SRG- N^3LO NN-only (dots), NN+NNN-induced (dashed line) and SRG- $(\text{N}^3\text{LO NN} + \text{N}^2\text{LO NNN})$ interactions (solid line) with $\Lambda = 2.0 \text{ fm}^{-1}$ obtained within the HO basis size $N_{\max} = 11$ and frequency $\hbar\Omega = 20$ MeV. See also the caption of Fig. 5.

and overall such a procedure led to (never obtained before) realistic results. However, a truly accurate *ab initio* description demands the inclusion of both induced and chiral NNN interactions.

While the inclusion of the NNN force into the NCSM/RGM formalism is conceptually straightforward, in practice it poses major challenges having to deal with: 1) the large number of NNN matrix elements, which makes it essential to work within the JT-coupled scheme; and 2) the appearance of kernels depending on the three-body densities of the target already for nucleon-nucleus processes, which demands new efficient computing strategies for applications with p -shell targets to be possible. Figures 5 and 6 present initial results for ${}^4\text{He}(n, n){}^4\text{He}$ scattering phase shifts with inclusion of the NNN force. The use of SRG-evolved interactions facilitates the convergence of the calculation within $N_{\max} \sim 11$. At the same time, Fig. 6 highlights the influence of induced and initial components of the NNN force on the resonant phase shifts. The largest splitting between ${}^2P_{3/2}$ and ${}^2P_{1/2}$ is found when both induced and chiral NNN forces are included (NN+NNN curve). It should be noticed that these results are still preliminary, as not all relevant excitations of the ${}^4\text{He}$ nucleus have been taken into account yet. In particular, the resonances are sensitive to the inclusion of the first six excited states of the ${}^4\text{He}$ [2] (here only the g.s. is included). We will complete this study in the coming months.

We have also obtained first results for the $d+{}^4\text{He}$ scattering phase shifts and the ground state of ${}^6\text{Li}$ including both SRG-induced and chiral NNN forces. The model spaces adopted so far contain only the g.s. of the ${}^4\text{He}$ and d nuclei within a $N_{\max} = 8$ HO basis size. While calculations for larger N_{\max} values and including pseudo-excited states of the deuteron (fundamental to model the deformation and virtual breakup of this nucleus) are under way, these preliminary results are already very promising. In particular, the inclusion of the NNN force produces a change in position and splitting of the 3D_1 and 3D_2 scattering phase shifts, which were not well described in our former calculation with only the NN part of the SRG

interaction. The NNN force has also the effect of increasing the binding energy of the ${}^6\text{Li}$ nucleus.

4.2 Three-cluster dynamics

A proper description of Borromean halo nuclei and three-body breakup reactions (but also virtual breakup effects) within the NCSM/RGM approach requires the inclusion of three-cluster channel states and the treatment of the three-body dynamics. At present we have completed the development of the formalism for the

Table 1 Ground-state energies of the ${}^4,6\text{He}$ nuclei in MeV. Both NCSM/RGM and NCSM calculations were performed with the SRG- $N^3\text{LO}$ NN potential with $\Lambda = 1.5 \text{ fm}^{-1}$, and $\hbar\Omega = 16 \text{ MeV}$ HO frequency. Extrapolations were performed with an exponential fit.

Approach		$E_{g.s.}({}^4\text{He})$	$E_{g.s.}({}^6\text{He})$
NCSM/RGM	($N_{\text{max}} = 12$)	-28.22 MeV	-28.72 MeV
NCSM	($N_{\text{max}} = 12$)	-28.22 MeV	-29.75 MeV
NCSM	(extrapolated)	-28.23 MeV	-29.80 MeV

treatment of three-cluster systems formed by two separate nucleons in relative motion with respect to a nucleus of mass number $A - 2$. Preliminary results for the g.s. energy of ${}^6\text{He}$ within a ${}^4\text{He}(\text{g.s.})+n+n$ cluster basis and an $N_{\text{max}} = 12$, $\hbar\Omega = 16 \text{ MeV}$ HO model space, are compared to NCSM calculations in Table 1. The interaction adopted is the SRG- $N^3\text{LO}$ NN potential with $\Lambda = 1.5 \text{ fm}^{-1}$. With such a low value of Λ , at $N_{\text{max}} \sim 12$ the binding energy calculations are close to convergence in both NCSM/RGM and NCSM approaches. The $\sim 1 \text{ MeV}$ difference observed is due to the excitations of the ${}^4\text{He}$ core, included only in the NCSM at present. Contrary to the NCSM, in the NCSM/RGM the ${}^4\text{He}(\text{g.s.})+n+n$ wave functions present the appropriate asymptotic behavior. This will be essential in describing ${}^6\text{He}$ excited states in the continuum, such as, *e.g.* the 1^- soft dipole resonance. Work towards the solution of the three-cluster NCSM/RGM equations with continuum boundary conditions is under way.

5 Conclusions

We presented an outline of the NCSM/RGM, an *ab initio* many-body approach capable of describing simultaneously both bound and scattering states in light nuclei, by complementing the RGM with the use of realistic interactions, and a microscopic and consistent description of the nucleon clusters, obtained via the *ab initio* NCSM. We discussed applications to fusion reactions that power stars and Earth based fusion facilities, such as the ${}^7\text{Be}(p,\gamma){}^8\text{B}$ radiative capture, and the ${}^3\text{H}(d,n){}^4\text{He}$ and ${}^3\text{He}(d,p){}^4\text{He}$ fusion reactions. Finally, we outlined the progress toward the inclusion of the NNN force into the formalism and the treatment of three-cluster dynamics, and presented an initial assessment of NNN -force effects on ${}^4\text{He}(n,n){}^4\text{He}$ scattering, as well as preliminary results for the g.s. energy of ${}^6\text{He}$ computed within a ${}^4\text{He}(\text{g.s.})+n+n$ NCSM/RGM three-cluster basis. Since

the publication of the first results [1, 2, 5], obtained for nucleon-nucleus collisions, the NSCM/RGM has grown into a powerful approach for the description of binary reactions starting from realistic NN forces. A truly accurate *ab initio* description of light-ion fusion reactions and light exotic nuclei that encompasses the full NNN force and the three-cluster dynamics is now within reach.

References

1. S. Quaglioni, P. Navrátil, Phys. Rev. Lett. **101**, 092501 (2008)
2. S. Quaglioni, P. Navrátil, Phys. Rev. C **79**, 044606 (2009)
3. P. Navrátil, J.P. Vary, B.R. Barrett, Phys. Rev. Lett. **84**, 5728 (2000)
4. P. Navrátil, S. Quaglioni, Phys. Rev. C **83**, 044609 (2011)
5. P. Navrátil, R. Roth, S. Quaglioni, Phys. Rev. C **82**, 034609 (2010)
6. P. Navrátil, R. Roth, S. Quaglioni, Physics Letters B **704**(5), 379 (2011)
7. P. Navrátil, S. Quaglioni, Phys. Rev. Lett. **108**, 042503 (2012)
8. S.K. Bogner, R.J. Furnstahl, R.J. Perry, Phys. Rev. C **75**, 061001 (2007)
9. R. Roth, S. Reinhardt, H. Hergert, Phys. Rev. C **77**, 064003 (2008)
10. D.R. Entem, R. Machleidt, Phys. Rev. C **68**, 041001 (2003)
11. R. Roth, P. Navrátil, Phys. Rev. Lett. **99**, 092501 (2007)
12. R. Roth, Phys. Rev. C **79**, 064324 (2009)
13. E.D. Jurgenson, P. Navrátil, R.J. Furnstahl, Phys. Rev. Lett. **103**, 082501 (2009)
14. E.D. Jurgenson, P. Navrátil, R.J. Furnstahl, Phys. Rev. C **83**, 034301 (2011)
15. F. Schümann, et al., Phys. Rev. Lett. **73**, 232501 (2003); Phys. Rev. C **73**, 015806 (2006).
16. A.R. Junghans, et al., Phys. Rev. C **68**, 065803 (2003)
17. E. Adelberger, et al., Rev. Mod. Phys. **83**, 195 (2011); Rev. Mod. Phys. **70**, 1265 (1998).